

June 17-18, 2009, Delft, The Netherlands

Recent advances in masonry homogenization

P.B. Lourenço

ISISE, University of Minho, Portugal

G. Milani

Politecnico di Milano, Italy

A. Zucchini

ENEA, Italy

Keywords: Micro-mechanics, limit analysis, orthotropic failure envelop, validation

1 INTRODUCTION

Homogenization remains a popular subject in masonry research. Usually the complex geometry of the basic cell is replaced by a simplified geometry so that a close-form solution of the homogenization problem is possible. Many other approaches involving different approximations and ingenious assumptions have been sought. To overcome the weak approximation, a micro-mechanical homogenization model that consider additional internal deformation mechanisms and a model based on the polynomial expansion of the stress field inside the R.V.E. are presented.

2 A MICRO-MECHANICAL HOMOGENIZATION APPROACH

As a consequence of the differences in stiffness between units and mortar, a complex interaction between the two masonry components occurs when masonry is deformed. The differences in stiffness cause an unequal distribution of deformations over units and mortar, compared with the average deformation of masonry composite. As a result the individual (internal) stresses of units and mortar deviate from the average (external) stresses of the composite. The elastic mechanical properties of an orthotropic material equivalent to a basic masonry cell can be derived from a suitable micromechanical model with appropriate deformation mechanisms, which take into account the staggered alignment of the units in a masonry wall. The unknown internal stresses and strains can be found from equilibrium equations at the interfaces between the basic cell components, from a few ingenious assumptions on the kinematics of the basic cell deformation and by forcing the macro-deformations of the model and of the homogeneous material to contain the same strain energy. This homogenisation model has been extended, by coupling the elastic micro-mechanical model with a damage model for joints and units by means of an iterative solution procedure to calculate the damage coefficients. A simple isotropic damage model with only one single parameter has been utilized, because the discrete internal structure of the cell, and implicitly its global anisotropic behaviour, is taken into account by the three-dimensional micromechanical model.

When the basic cell is loaded only with normal stresses, the micromechanical model assumes that all shear stresses and strains inside the basic cell can be neglected, except the in-plane shear stress and strain (σ_{xy} and ϵ_{xy}) in the bed joint and in the unit. The non-zero stresses and strains in the bed joint, head joint and unit are assumed to be constant, with the exception of the normal stress σ_{xx} in the unit, which is a linear function of x and accounts for the effect of the shear σ_{xy} in the bed joint, and with the exception of the shear stress σ_{xy} in the unit, which is linear in y . The coupling of this model with non-linear constitutive models, leads to an iterative algorithm,

in which at each cycle a system of equilibrium equations is solved to obtain the unknown effective stresses and strains.

The model was applied to a real masonry basic cell and compared with the results of an accurate finite element analysis (FEA) under linear elastic analysis. In the finite element analysis and the analytical model, the properties of the components can be taken absolutely equal. Different stiffness ratios between mortar and unit are considered. The material properties of the unit are kept constant, whereas the properties of the mortar are varied to yield a ratio E_b / E_m ranging from 1 to 1000. The adopted range is very large, if only linear elastic behaviour of mortar is considered. However, those high values are indeed encountered if inelastic behaviour is included. In such case, E_b and E_m should be understood as linearised tangent Young's moduli, representing a measure of the degradation of the (tangent / secant) stiffness matrices utilised in the numerical procedures adopted to solve the non-linear problem. Note that the ratio E_b / E_m tends to infinity when softening of the mortar is complete and only the unit remains structurally active. The elastic properties of the homogenised material, calculated by means of the proposed micro-mechanical model, are compared in Figure 1a with the values obtained by FE analysis. The agreement is very good in the entire range $1 \leq E_b / E_m \leq 1000$, with a maximum error $\leq 6\%$. A comparison between the results obtained with the micro-mechanical model and experimental results is given in Figure 1b. Very good agreement is found in the shape of the yield surface, indicating that the proposed model can be used as a possible macro-model to represent the composite failure of masonry.

Figure 2 shows the validation of the model under non-linear uniaxial loading. The algorithm has been tested in the fracture problem of an infinitely long wall under tensile loading parallel to the bed joint (Figure 2a). The model reproduces with good agreement the FE analysis of the cell degradation and the two peaks of the failure load for a zero dilatancy angle in the joints. The head joint is the first to fail in tension and the bed joint takes its place in the load carrying mechanism of the cell. The load is transferred through bed joint shear from unit to the other, with the cell showing regained elastic behaviour for increasing loads, until final failure of the bed joint in shear. The residual load carrying capacity is zero because there is no vertical compression, and therefore no friction effect.

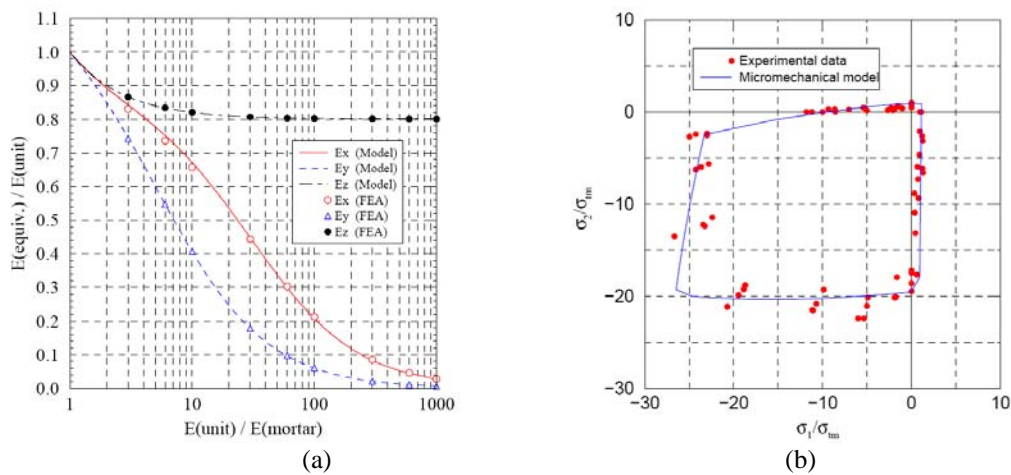


Figure 1. Elastic results for the micro-mechanical model: (a) comparison of Young's moduli with FEA results for different stiffness ratios; (b) comparison with experimental results of Page (1981,1983).

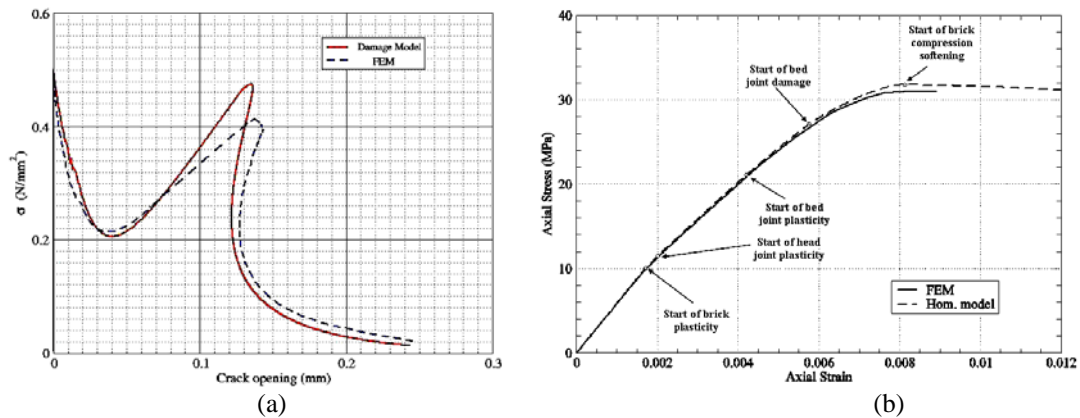


Figure 2. Inelastic response of the model: (a) post-peak tensile behaviour and comparison with FEM results; (b) axial stress vs. axial strain and comparison between finite element simulation.

Figure 2b shows the behaviour of a basic masonry cell under axial compressive loading perpendicular to the bed joint and a comparison with an accurate FE calculation. The curves obtained with the homogenisation model almost coincide with the corresponding FE results, with marginal computational effort and no convergence difficulties. For weak mortars the plastic flow of the mortar joints starts very early in the loading path, while the brick non-linear behaviour begins a little later. The brick is in a tension-compression-tension state, while the mortar is in a tri-axial compression state for the lateral containment effect of the stiffer brick. The head joint suffers some negligible damage in tension just before the complete failure of the brick in tension, which leads to the catastrophic failure of the entire cell. For strong mortars the plastic flow starts earlier in the brick than in the bed joint, due to the higher strength of the mortar. The inversion of the elastic mismatch between mortar and brick in this case (the mortar is much stiffer than the brick) yields in this case a tension-tension-compression state of the bed joint. A substantial (57%) isotropic damage in tension is reached in the bed joint, but the failure of the masonry cell is driven again by the crushing of the brick. The damage of the mortar in the bed is due to the high tension in the x and z direction.

3 A STRESS FIELD EXPANSION APPROACH

Using the lower bound theorem of limit analysis and the hypotheses of homogenization, a solution for the homogenization problem can be derived by means of a (non-linear) optimization problem. Here, the masonry cell is sub-divided into thirty-six sub-domains and, for each sub-domain, polynomial distributions of cubic degree are assumed for the stress components.

In Figure 3a,b the principal stress distribution at collapse from the lower bound analysis and the velocities at collapse from the upper bound analysis are reported. Good agreement is found among the model here proposed and experimental data. Finally, in Figure 3c a comparison between the numerical failure loads provided respectively by the lower and upper bound approaches and the experimental load-displacement diagram is reported. Collapse loads $P(-) = 210$ kN and $P(+) = 245$ kN are numerically found using a model with 288 triangular elements, whereas the experimental failure shear load is approximately $P = 250$ kN.

The homogenized model is also employed in order to reproduce experimental data for panels out-of-plane loaded. Figure 4a shows typical comparisons between experimental pressure-displacement curves, numerical pressure-displacement curves obtained by means of an orthotropic elasto-plastic macro-model and the results with the proposed formulation. Figure 4b shows results of the numerical analysis in terms of ultimate principal moment distribution and failure mechanisms. The agreement with experimental results is worth noting in all cases analysed. Finally, some real scale application of the model to a building in Italy is shown in Figure 4c, demonstrating the possibility of using the proposed tools for safety evaluation. In this case, a complex collapse mechanism involving piers and walls has been found.

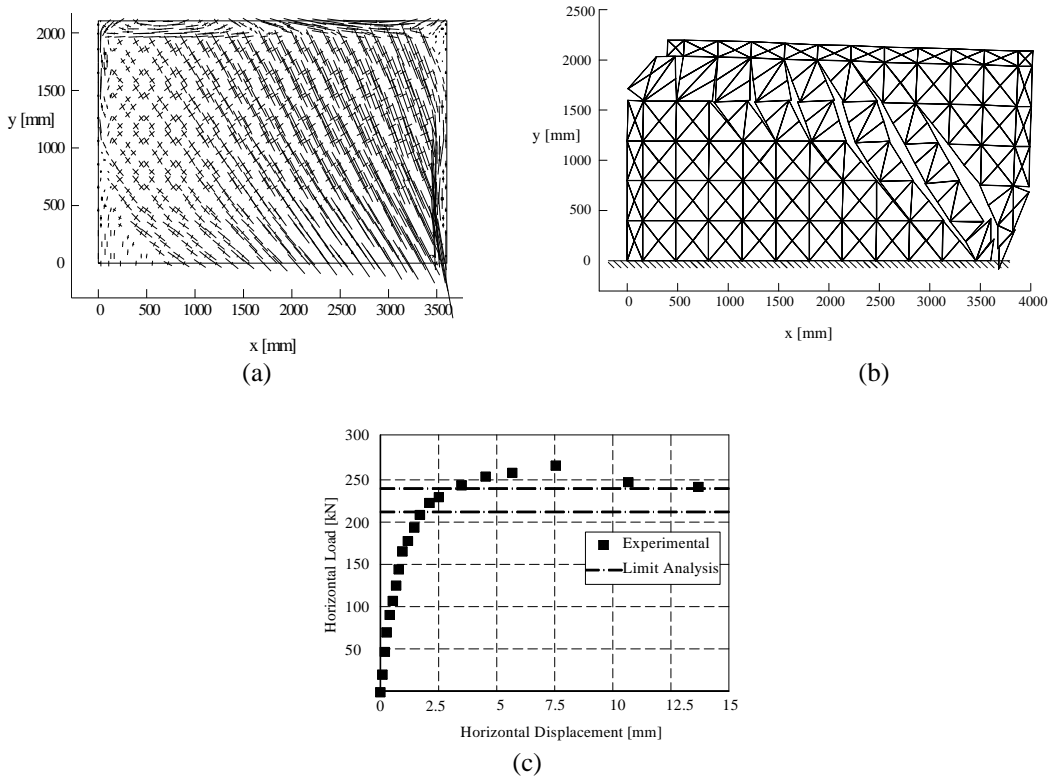


Figure 3. Shear wall: (a) Principal stress distribution at collapse, lower bound; (b) Velocities at collapse, upper bound; (c) Comparison between experimental load-displacement diagram and limit analysis.

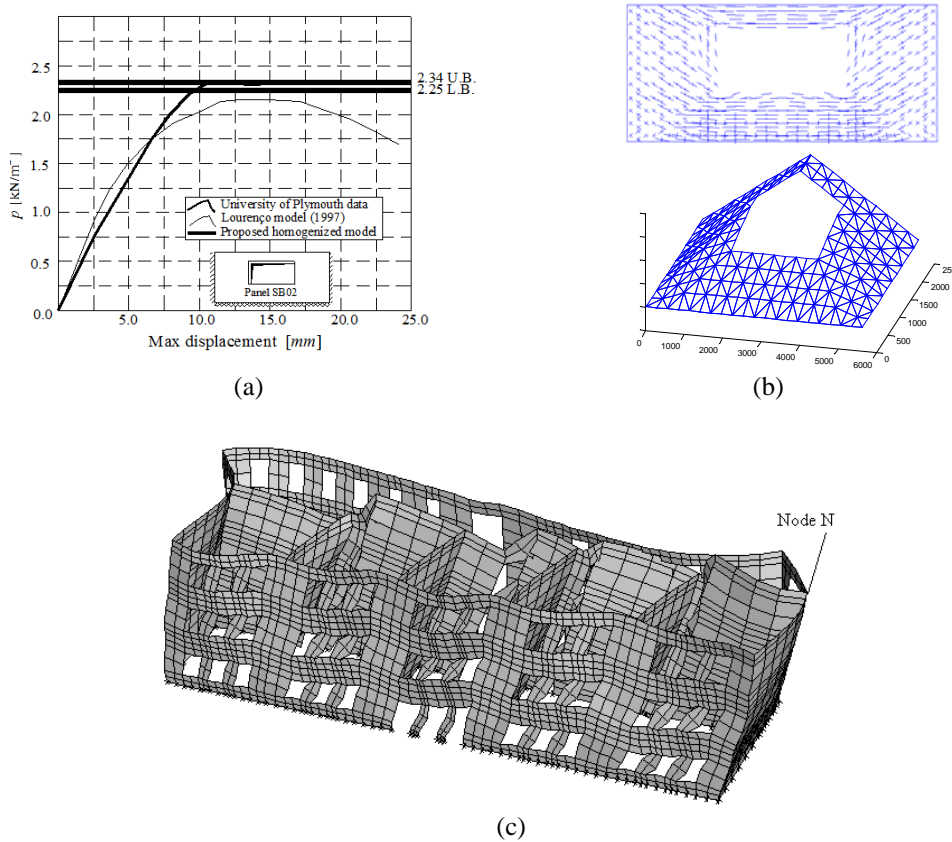


Figure 4. Results involving out-of-plane loading: (a) comparison between experimental and numerical results for masonry wall subjected to out-of-plane loading; (b) lower (principal moments at collapse) and upper bound results (deformed mesh at collapse and yield line pattern) for the same wall; (c) collapse of a masonry building subjected to earthquake action.

4 RELATED PAPERS

Overview

- [1] Lourenço, P.B., Milani, G., Tralli, A., Zucchini, A., Analysis of masonry structures: review of and recent trends of homogenisation techniques, *Canadian Journal of Civil Engineering*, 34 (11), p. 1443-1457 (2007)

Micro-mechanical model

- [2] Zucchini, A., Lourenço, P.B., Mechanics of masonry in compression: Results from a homogenisation approach, *Computers & Structures*, 85(3-4), p. 193-204 (2007)
- [3] Zucchini, A., Lourenço, P.B., A coupled homogenisation-damage model for masonry cracking, *Computers & Structures*, 82, p. 917-929 (2004)
- [4] Zucchini, A., Lourenço, P.B., A micromechanical model for the homogenisation of masonry, *Int. J. Solids and Structures*, 39(12), p. 3233-3255 (2002)

Finite element limit analysis

- [5] Milani, G., Lourenço, P.B., Blast analysis of enclosure masonry walls using homogenization approaches, *International Journal for Multiscale Computational Engineering* (accepted for publication) (January, 2009)
- [6] Milani, G., Lourenço, P.B., A simple discontinuous upper bound limit analysis approach with sequential linear programming mesh adaptation, *International Journal of Mechanical Sciences*, 51(1), p. 89-104 (2009)
- [7] Milani, G., Lourenço, P.B., Tralli, A., 3D Homogenized limit analysis of masonry buildings under horizontal loads, *Engineering Structures*, 29(11), p. 3134-3148 (2007)
- [8] Milani, G., Lourenço, P.B., Tralli, A., A homogenization approach for the limit analysis of out-of-plane loaded masonry walls, *J. Struct. Engrg., ASCE*, p. 1650-1663 (2006)
- [9] Milani, G., Lourenço, P.B., Tralli, A., Homogenised limit analysis of masonry walls. Part I: Failure surfaces, *Computers & Structures*, 84(3-4), p. 166-180 (2006)
- [10] Milani, G., Lourenço, P.B., Tralli, A., Homogenised limit analysis of masonry walls. Part II: Structural applications, *Computers & Structures*, 84(3-4), p. 181-195 (2006)